Published in final edited form as:
Exp Mol Pathol. 2012 August ; 93(1): 173–181. doi:10.1016/j.yexmp.2012.04.021.

Sirolimus modulates HIVAN phenotype through inhibition of epithelial mesenchymal transition

Anju Yadav, **Dileep Kumar**, **Divya Salhan**, **Rungwasee Rattanavich**, **Subani Maheshwari**, **Madhuri Adabala**, **Guohua Ding**, and **Pravin C. Singhal**
[1]Immunonlogy Center, Feinstein Institute for Medical Research, North Shore-Long Island Jewish Health System, Manhasset, NY 11030

Abstract

HIV-associated nephropathy (HIVAN) is characterized by proliferative phenotype in the form of collapsing glomerulopathy and microcystic dilatation of tubules. Recently, epithelial mesenchymal transition (EMT) of renal cells has been demonstrated to contribute to the pathogenesis of proliferative HIVAN phenotype. We hypothesized that sirolimus would modulate HIVAN phenotype by attenuating renal cell EMT. In the present study, we evaluated the effect of sirolimus on the development of renal cell EMT as well as on display of HIVAN phenotype in a mouse model of HIVAN (Tg26). Tg26 mice receiving normal saline (TgNS) showed enhanced proliferation of both glomerular and tubular cells when compared to control mice-receiving normal saline (CNS); on the other hand, Tg26 mice receiving sirolimus (TgS) showed attenuated renal cell proliferation when compared with TgNS. TgNS also showed increased number of α-SMA-, vimentin-, and FSP1- positive cells (glomerular as well as tubular) when compared with CNS; however, TgS showed reduced number of SMA, vimentin, and FSP1 +ve renal cells when compared to TgNS. Interestingly, sirolimus preserved renal epithelial cell expression of E-cadherin in TgS. Since sirolimus attenuated renal cell ZEB expression (a repressor of E-cadherin transcription), it appears that sirolimus may be attenuating renal cell EMT by preserving epithelial cell E-cadherin expression.

HIV-associated nephropathy (HIVAN) is the most common cause of chronic kidney disease in HIV-1 sero-positive patients (Szczech et al., 2004). It is caused by combination of genetic, environmental, and specific host factors (Marras et al., 2002; Kimmel et al., 2003; Kopp et al., 2008; Papeta et al., 2009). It predominantly occurs in patients with African-

Address for correspondence: Pravin C. Singhal, M.D., Division of Kidney Diseases and Hypertension, 100 Community Drive, Great Neck, NY 11021, Tel 516-465-3010, Fax 516-465-3011, singhal@lij.edu.

Contribution of the authors
Anju Yadav Carried out the experiments
Dileep Kumar. Carried out the experiments
Divya Salhan Carried out the experiments
Rungwasee Rattanavich carried out experiments
Subani Maheshwari carried out the experiments
Madhuri Adabala carried out the experiments
Guohua Ding analysed renal pathology
Pravin C. Singhal designed the experiments and written the manuscript

This work was presented at the 41st Annual Meeting of the American Society of Nephrology on November 11th, at the Pennsylvania Convention Center, Philadelphia, PA.

America descent. The genetic factors responsible for the susceptibility of HIVAN in this population include Apol1 gene (Papeta et al., 2011). Interestingly, this gene induces susceptibility for the development of focal segmental glomerulosclerosis (FSGS) not only in HIVAN but also in other disease models of FSGS- hypertension and diabetes (Freedman et al., 2010). In HIVAN, both podocytes and tubular cells have been reported to be infected by HIV-1 (Marras et al., 2002; Kimmel et al., 2003). Renal cell dysfunction has been attributed to viral gene expression by these cells in a dysregulated milieu of phologogenic host factors (Barisoni et al., 1999).

HIVAN is characterized by unique combination of glomerular and tubular proliferative epithelia (Rao et al., 1987). Glomerular lesions manifest predominantly as collapsing variant of FSGS, whereas, tubular lesions are characterized by cystic dilatation. To study HIVAN, several animal models mimicking HIVAN have been described (Kopp et al, 1992; Zhong et al., 2005; Lu et al., 2006). The first and the most commonly studied model is Tg26 mouse model, which carries a transgene with a modified replicative-inactive HIV-1 provirus (Lu et al., 2006). These animals develop proteinuria at the age of four weeks and renal lesions are characterized by collapsing glomerulosclerosis and microcystic dilatation of tubules and thus mimicking human disease model (Kopp et al., 1992).

Podocytes are terminally differentiated cells and therefore they do not proliferate in response to podocyte injury (Stokes et al., 2006). However, podocyte proliferation has been considered to be a characteristic feature of collapsing variant of FSGS (Stokes et al., 2006). On the other hand, some investigators demonstrated that parietal cells also contributed to prolifeative HIVAN phenotype (Dijkman et al., 2006). Recently, a role of myofibroblasts has been demonstrated in the manifestation of both glomerular and tubular cell proliferative phenotype in HIVAN (Yadav et al., 2010). However, the lineage of myofibroblasts was not studied in these studies. Moreover, kidney has both resident and migrated population of macrophages which may also be displaying EMT markers.

Epithelial mesenchymal transition (EMT) is a process in which renal epithelial cells lose their epithelia phenotype and attain new characteristic features of mesenchymal cells (Hay and Zuk, 1995; Grootecclaes and Frisch, 2000; Guaita et al., 2002). This process is fundamentally linked to generation of myofibroblasts (matrix-producing fibroblasts). EMT of tubular epithelial cells has been demonstrated to be the common mode for the progression of tubulointerstitial fibrosis (Lan, 2003; Li et al., 2003). Once renal epithelial cells are transdedifferentiated into myofibroblasts, they migrate, proliferate, and synthesize matrix, leading to renal fibrosis.

EMT has been reported to contribute to the progression of renal fibrosis in animal models of anti-glomerular basement membrane (GBM) glomerulonephritis, diabetic nephropathy, renal ablation model, and nephrotoxic serum nephritis (Ng et al., 1998, 1999; Odfield et al., 2001). Recently, occurrence of EMT has been demonstrated during the development of glomerular proliferative phenotype in HIVAN (Yadav et al., 2010). Occurrence of EMT in glomerular epithelia leading to glomerulosclrosis has added a new paradigm in the pathogenesis of HIVAN.

Ang II has been demonstrated to play an important role in the initiation of tubular cell EMT both in animal and human experimental kidney disease models (Youhua, 2004;Wolf, 2006). Moreover, both the production and the blockade of the effect of Ang II have been used to slow down the progression of HIVAN both in human and animal experimental animal models (Burns et al, 1997; Bird et al., 1998; Hiramatsu et al., 2007). However, in these studies the role of Ang II in the development of renal cell EMT was not evaluated. Interestingly, telmisartan, an Ang II type 1 (AT1) receptor blocker has been demonstrated to

attenuate EMT in a mouse model of HIVAN (Yadav et al., 2010). On that account, we hypothesized that the blockade of EMT could be used as a therapeutic strategy to modulate the development of HIVAN.

Recently, sirolimus has been demonstrated to inhibit the development as well as progression of EMT in a mouse UUO model (Wu et al., 2006). In this model sirolimus not only inhibited renal cell EMT but also slowed progression of tubulointerstitial fibrosis. These investigators suggested using sirolimus as a therapeutic tool in renal diseases progressing as the result of progressive tubulointerestitial fibrosis.

In the present study, we evaluated the effect of sirolimus on the modulation of renal cell EMT in HIVAN (Tg26) mice. We observed that sirolimus not only attenuated the development of renal cell EMT but also inhibited the display of HIVAN phenotype. These studies provide insight into the development and progression of both glomerulosclerosis and tubulointerstitial fibrosis in patients with HIVAN.

Material and Methods

HIV transgenic mice

We have used age and sex matched FVB/N (control) and Tg26 (on FVB/N background). Breeding pairs of FVB/N were obtained from Jackson Laboratories (Bar Harbor, ME). Breeding pairs to develop Tg26 colonies were kindly gifted by Prof. Paul E. Klotman M.D., Chairman, Department of Medicine, Mount Sinai Medical Center, New York, NY). Mice were housed in groups of 4 in a laminar-flow facility (Small Animal Facility, Long Island Jewish Medical Center, New Hyde Park, NY). Tg26 mice develop proteinuria and renal lesions at 4 weeks. The Ethics Review Committee for Animal Experimentation of Long Island Jewish Medical Center approved the experimental protocol.

Experimental studies

Age (three weeks old) and sex matched Tg26 mice in groups of six were administered ether normal saline (TgNS) or sirolimus (5 mg/Kg every other day, TgS, intraperitoneal) for either two weeks (protocol A) or eight weeks (Protocol B). Age and sex matched FVBN mice in groups of six were also administered either normal saline (intraperitoneal, CNS) or sirolimus (5 mg/Kg every other day, intraperitoneal, CS) for the same duration. These animals served as control for TgNS and TgS animals. At the end of the scheduled periods, the animals were anesthetized (by inhalation of isoflurane and oxygen) and sacrificed (by a massive intraperitoneal dose of sodium pentobarbital). After euthanization, blood was collected by a cardiac puncture. Both kidneys were excised; one was processed for histological and immunohistochemical studies while the other was used for RNA and protein extraction. Three-micrometer sections were prepared and stained with hematoxylin-eosin and periodic-acid Schiff.

Immunohistochemical staining

The immunohistochemistry protocol has been previously described (Yadav et al., 2010). Briefly, the sections were de-paraffinized and antigen retrieval was accomplished by microwave heating for 10 minutes at maximum output in 10 mM citrate buffer (pH 6.0). The endogenous peroxidase activity was blocked with 0.3% hydrogen peroxide in methanol for 30 minutes at room temperature (RT). Sections were washed in phosphate buffered saline (PBS) thrice and incubated in blocking serum solution according to the primary antibody for 1 hour at RT. The primary antibody was applied in different dilutions: PCNA (mouse monoclonal, dilution 1:500; Santa Cruz Biotechnology, Santa Cruz, CA), α-SMA (monoclonal mouse anti-human, dilution 1:200, Dako, Denmark), FSP-1 (anti S-100A4,

rabbit polyclonal, dilution 1:150, Sigma, MO), vimentin (monoclonal mouse, 1:400, Santa Cruz), E-cadherin (mouse monoclonal, dilution, 1:400, Santa Cruz Biotechnology, CA), or ZEB (rabbit polyclonal, dilution, 1.200, Abcam, Cambridge, MA), and then incubated overnight at 4°C in a humidifying chamber. Each of the sections were washed thrice with PBS and incubated in the appropriate secondary antibody at 1:250 dilutions at RT for 1 hour. After washing with PBS three times, sections were incubated in ABC reagent (Vector Laboratories, Burlingame, CA) for 30 minutes. Sections were washed thrice in PBS and placed in VECTOR Nova RED substrate kit SK-4800 (Vector Laboratories, Burlingame, CA) followed by counterstaining with methyl green. The sections were then dehydrated and mounted with a xylene-free mounting media (Permount, Fisher Scientific Corporation, Fair Lawn, NJ). In all the batches of immunostaining, appropriate positive and negative controls were used.

All the immune-stained slides were coded and blindly studied by a semiquantitative grading score. Since stained periglormerular (PGCs) and peritubular cells (PTCs), especially in TgNS, were in contiguity with the glomerular epithelial cells (parietal and visceral, PECs) and tubular cells (TCs), we have counted PGCs and PTCs together with PECs and TCs, respectively. Number of positively stained cells was counted per tubule as well as per glomerulus in 10 random fields in each labeled renal cortical section (under 20X lens). Positive staining was characterized by distinctly greater nuclear/cytoplasmic staining from the background staining of that cortical section; moreover, positive cellular staining had to be accompanied with distinctly greater nuclear/cytoplasmic staining of cells when compared with cortical sections labeled with only secondary antibody (without primary antibody).

Protein extraction and Western blotting

Renal cortical tissue were mixed with lysis buffer (1× PBS, pH 7.4, 0.1% SDS, 1% NP-40, 0.5% sodium deoxycholate, 1.0 mM sodium orthovanadate, 10 μ1 of protease inhibitor cocktail, 100X (Calbiochem) per one ml of buffer, and 100 μg/ml PMSF), homogenized with a dounce homogenizer and then incubated on ice for 30 min. The samples were subjected to centrifugation at 15,000g for 20 min at 4°C. The collected supernatant was evaluated for protein concentration as determined by a BCA kit (Pierce, Rockford, IL). The proteins, 20–40 μg/lane, were separated by 10 or 12% sodium dodecyl sulfate-polyacrylamide gel electrophoresis and transferred onto a nitrocellulose membrane using a Bio-Rad Western blotting apparatus. After transfer, blots were stained with Ponceau S (Sigma, MO) to check for complete protein transfer and equal loading. The blots were blocked with 0.5% BSA and 0.1% TWEEN 20 in 1X PBS for 60 min at room temperature and then incubated with the PCNA (mouse monoclonal, 1:1000, Santa Cruz Biotechnology, CA) or α-SMA (mouse monoclonal, 1:1000, Dako, Denmark), FSP-1 (rabbit polyclonal, 1:1000, Sigma, MO) overnight at 4°C. A horseradish peroxidase-conjugated appropriate secondary antibody was applied for 1 hour at RT. The blots were then developed using a chemiluminescence detection kit (ECL, Amersham, Arlington Heights, IL) and exposed to Kodak X-OMAT AR film. To reassure equal loading of proteins, the blots were striped and reprobed for actin

Reverse Transcription PCR Analysis

Renal tissues from the protocol A (n=3) were studied for renal cell expression of PCNA, α-SMA, FSP1, and ZEB1. Renal tissues were harvested and RNA was extracted using TRIZOL (Invitrogen corp.). For cDNA synthesis, 2 μg of the total RNA was preincubated with 2 nmol of random hexamer (Invitrogen Corp) at 65°C for 5 min. Subsequently, 8ul of the reverse-transcription (RT) reaction mixture containing Cloned AMV RT, 0.5 mmol each of the mixed nucleotides, 0.01 mol dithiothreitol, and 1000 U/mL Rnasin (Invitrogen Corp) was incubated at 42°C for 50 min. For a negative control, a reaction mixture without RNA

or reverse transcription (RT) was used. Samples were subsequently incubated at 85°C for 5 min to inactivate the RT.

Quantitative PCR was carried out in an ABI Prism 7900HT sequence detection system using the primer sequences as shown below:

PCNA F: GGGTTGGTAGTTGTCGCTGT

R: AGCACCTTCTTCAGGATGGA

SMA F: CTGACAGAGGCAACCACTGAA

R: CATCTCCAGAGTCCAGCACA

FSP-1 F: GATGAGCAACTTGGACAGCA

R: ATGTGCGAAGAAGCCAGAGT

ZEB-1 F: TGCACTGAGTGTGGAAAAGC

R: TGGTGATGCTGAAAGAGACG

SYBR green was used as the detector and ROX as the passive reference gene. Results (means ± S.D.) represent three animals as described in the legend. The data was analyzed using the Comparative C_T method ($\Delta\Delta^{CT}$ method). Differences in C_T are used to quantify relative amount of PCR target contained within each well. The data was expressed as relative mRNA expression in reference to control, normalized to quantity of RNA input by performing measurements on an endogenous reference gene, GAPDH. A representative gel electrophoresis was also carried out with alpha tubulin as the house keeping gene. After agarose gel electrophoresis, a Polaroid Camera System was used to capture images. Image J (Research Services Branch, National Institutes of Health, Bethesda, MD) was used to carry out densitometric analysis of RT-PCR gels.

Statistical analysis

For comparison of mean values between two groups, the unpaired t test was used. To compare values between multiple groups, analysis of variance (ANOVA) was applied and a Bonferroni multiple range test was used to calculate a p-value. Statistical significance was defined as $P<0.05$.

Results

Since the outcomes in the protocols A and B were similar, we have presented the data of the porotocol A only.

Sirolimus attenuates renal cell proliferative phenotype in HIVAN mice

To determine the proliferation profile of renal cells, renal cortical sections from six CNS, CS, TgNS, and TgS from the protocol A and B were immunolabeled for PCNA. Representative microphotographs of cortical sections immunolabeled for PCNA from CNS, TgNS, and TgS (protocol A) are shown in Fig 1A. Since PCNA +ve periglormerular (PGCs) and peritubular cells (PTCs) especially in TgNS were in contiguity with the glomerular epithelial cells (parietal and visceral, PECs) and tubular cells (TCs), we have counted PGCs and PTCs together with PECs and TCs, respectively. Cumulative data of mean number of proliferating (+ve PCNA) PECs-PGCs and TCs-PTCs are shown in Fig. 1B (Protocol A). As shown in Fig 1B, TgNS mice showed five-fold increase ($P<0.001$) in the numbers of proliferating PECs-PGCs/glomerulus (n=100) when compared with CNS. On the other hand, TgS showed 50% decrease ($P<0.01$) in the numbers of proliferating PECs-PGCs/glomerulus when compared with TgNS (Fig. 1B). Similarly, TgNS showed two-fold increase ($P<0.01$)

in the numbers of proliferating TCs-PTCs/tubule (n=200) when compared to CNS; whereas, TgS showed 50% reduction (P<0.01) in proliferating TCs-PTCs/tubule when compared with TgNS (Fig. 1C). Since there was no difference between CNS and CS in terms of morphologic and proliferation data, we have not shown any data on CS.

Cumulative data on renal cell proliferation in protocol B are shown in Figs. 1D and 1E. TgNS mice showed greater (P<0.001) number of proliferating PECs-PGCs/glomerulus when compared to CNS; whereas, TgS showed lower (P<0.01) number of proliferating PECs-PGCs/glomerulus when compared to TgNS (Fig. 1D). TgNS showed five-fold increase in the numbers (P<0.001) of proliferating TCs-PTCs/tubule when compared to CNS; however, TgS showed 75% diminution (P<0.01) in proliferating TCs-PTCs/tubule when compared to TgNS (Fig. 1E).

Renal tissues from TgNS showed enhanced (P<0.01) mRNA expression for PCNA by real time PCR (Fig. 1 F, lower panel, protocol A). Western blots prepared from renal cortical tissues of CNS, TgNS, and TgS (two mice in each group, protocol A) were also probed for PCNA. As shown in Fig. 1F (upper panel), renal tissues from TgNS showed enhanced expression of PCNA when compared with CNS and TgS.

Sirolimus diminishes renal cell expression of α-SMA in HIVAN mice

To determine the effect of sirolimus on the transition of epithelial cells to myofibroblasts in TgNS, renal cortical sections from CNS, TgNS, and TgS from the protocol A, were immunolabeled for α-SMA, a marker of myofibroblasts. Representative microphotographs of cortical sections immunolabeled for α-SMA from CNS, TgNS, and TgS are shown in Fig. 2A. Cumulative data of PECs-PGCs and TCs-PTCs expressing α-SMA are shown in Figs. 2 B and 2C. As shown in Fig 2B, TgNS showed six-fold increase (P<0.001) in the numbers of α-SMA expressing PECs-PGCs/glomerulus when compared with CNS; whereas, TgS showed 60% decrease (P<0.01) in the numbers of α-SMA expressing PECs-PGCs/glomerulus when compared with TgNS (Fig. 2B). Similarly, TgNS showed three-fold increase (P<0.001) in the numbers of α-SMA expressing TCs-PTCs/tubule when compared with CNS; however, sirolimus treatment reduced (P<0.001) the numbers of α-SMA expressing TCs-PTCs/tubule by 80% (Fig 2C).

Cumulative data on renal cell α-SMA expression in protocol B is shown in Figs. 2D and 2E. TgNS mice showed greater (P<0.001) number of α-SMA +ve PECs-PGCs/glomerulus when compared to CNS; whereas, TgS showed lower (P<0.05) number of α-SMA +ve PECs-PGCs/glomerulus when compared to TgNS (Fig. 2D). TgNS showed five-fold increase in the numbers (P<0.05) of α-SMA +ve TCs-PTCs/tubule when compared to CNS; however, TgS showed 75% diminution (P<0.05) in α-SMA +ve TCs-PTCs/tubule when compared to TgNS (Fig. 2E). Since there was no difference between CNS and CS in terms of morphologic and α-SMA +ve cell count, we have not shown any data on CS.

Renal tissues from TgNS showed enhanced (P<0.01) mRNA expression for α-SMA by real time PCR studies (Fig. 2F, lower panel; protocol A). Similarly, in Western blotting studies, renal tissues from TgNS showed enhanced expression of α-SMA when compared with CNS and TgS (Fig. 2F, upper panel).

Sirolimus reduces renal cell expression of FSP-1 in HIVAN mice

To determine the effect of sirolimus on the transition of renal epithelial cells to fibroblasts in HIVAN mice, renal cortical sections from CNS, TgNS, and TgS from the protocol A, were immunolabeled for FSP1, a marker of fibroblasts. Representative microphotographs of cortical sections immunolabeled for FSP1 from CNS, TgNS and TgS are shown in Fig. 3A. Cumulative data of PECs-PGCs and TCs-PTCs expressing FSP1 are shown in Figs. 3B and

3C. As shown in Fig. 3B, TgNS showed four-fold greater (P<0.001) number of PECs-PGCs/glomerulus expressing FSP1 when compared with CNS; whereas, TgS displayed 75% decrease (P<0.001) in the numbers of of PECs-PGCs/glomerulus expressing FSP1 when compared with TgNS (Fig. 3B). TgNS also showed three-fold increase in the numbers of FSP1 expressing TCs-PTCs/tubule when compared with CNS (P<0.01); however, sirolimus treatment reduced (P<0.01) the numbers of α-SMA expressing TCs-PTCs/tubule by 64% (Fig. 3C). Since there was no difference between CNS and CS in terms of morphologic and FSP1 +ve cell count, we have not shown any data on CS.

Renal tissues from TgNS showed enhanced (P<0.01) mRNA expression for FSP1 (Fig. 3D, protocol A) and ZEB1 (Fig. 3E, Protocol A) by real time PCR studies.

To quantify translation of renal tissue FSP1 and ZEB1 mRNA expression to respective proteins, immunoblots of renal tissues of CNS, TgNS, and TgS mice from the protocol A were probed for FSP1 and ZEB. The same blots were stripped and reprobed for actin. As shown in Fig. 3F, TgNS displayed enhanced expression of FSP1 as well as ZEB1. However, sirolimus inhibited increased expression of FSP1 and ZEB1.

Sirolimus allows preservation of expression of E-cadherin by renal cells in HIVAN mice

Renal epithelium is characterized by E-cadherin expression (36). To determine the effect of sirolimus on renal cell E-cadherin expression in HIVAN mice, renal cortical sections of CNS, TgNS, and TgS from the protocol A were labeled for E-cadherin. Renal cells of TgNS (Fig 4B) showed attenuated expression of E-cadherin when compared with CNS (Fig. 4A). However, treatment of HIVAN mice with sirolimus (TgS) allowed preservation of the expression of E-cadherin by renal cells (Fig. 4C).

Sirolimus attenuates renal cell vimentin expression in HIVAN mice

Vimentin is one of the markers for the mesenchymal transition (27). To confirm occurrence of renal cell EMT, renal cortical sections were immunolabeled for the expression of vimentin. Renal epithelial cells in TgS showed enhanced expression of vimentin (Fig 4E) when compared to both CNS (Fig. 4D) and TgS (Fig. 4F). These findings further confirm that renal cells were undergoing EMT in TgNS; however, occurrence of renal cell EMT was inhibited by sirolimus.

Sirolimus inhibits renal cell ZEB1/2 expression in HIVAN mice

To determine the involved mechanism for the sirolimus-induced preservation of E-cadherin expression by renal epithelial cells in HIVAN mice, we examined renal cell expression of ZEB, a transcriptional repressor of E-cadherin. Renal cortical sections of CNS, TgNS, and TgS were immunolabeled for ZEB1/2. As shown, in Fig 4H, TgNS showed enhanced expression of ZEB by renal cells. However, sirolmus attenuated renal cell expression of ZEB in HIVAN mice (Fig. 4I). To confirm this effect of sirolimus, RNA was isolated from renal cortical tissues of CNS, TgS, and TgS and the expression of ZEB1 was determined by real time PCR studies. TgNS showed enhanced (P<0.01) mRNA expression of ZEB1 (Fig. 3E). These findings indicate that preservation of renal cell expression of E-cadherin in TgS might have been contributed by diminished renal cell expression of ZEB1.

Discussion

In the present study, renal cortical sections of CNS and CS (control mice) showed only a small number of PCNA +ve glomerular and tubular cells; whereas, renal cortical sections of TgNS showed a greater number of PCNA +ve cells in both glomerular and tubular epithelia. However, sirolimus reduced the number of PCNA+ve glomerular and tubular cells in

HIVAN mice. Renal cortical sections of TgNS also showed a greater number of α-SMA- and FSP1 +ve cells (both glomerular and tubular); on the other hand, HIVAN mice-receiving sirolimus (TgS) displayed attenuated renal cell expression of both α-SMA and FSP1. Thus, it appears that sirolimus not only inhibited renal cell EMT but also attenuated the manifestation HIVAN phenotype. Since renal cell expression of ZEB1/2 has been implicated for diminished expression of E-cadherin (a marker of tubular epithelial cells) in renal cells of HIVAN mice (34), we examined the effect of sirolimus on renal cell ZEB1/2 expression in HIVAN mice. Interestingly, sirolimus receiving HIVAN mice (TgS) not only showed an attenuated renal cell expression of ZEB1/2 but also displayed an enhanced renal cell expression of E-cadherin. Since ZEB1 and 2 are repressors of mRNA transcription of E-cadherin, it appears that sirolimus may be providing the protection against EMT in HIVAN mice by preserving *de novo* epithelia characteristic- expression of E-cadherin.

Although the role of EMT in the development and progression of fibrosis in kidney disease has been increasingly recognized yet still being debated (Zeisberg and Duffield, 2010). Inflammatory milieu has been reported to invoke EMT in adult tubular epithelial cells in majority of the studies (Zeisberg and Neilson, 2009; Zeisberg and Duffield, 2010). However, occurrence of mesenchymal phenotype was identified by cellular expression of αSMA and FSP1 (Kalluri and Weinberg 2009; Zeisberg and Neilson, 2009; Zeisberg and Duffield, 2010). Since both α-SMA and FSP1 lack cell specificity and constancy of expression, they are not considered to be unequivocal markers of specific lineage; moreover, FSP1 expression in several tissues including injured kidneys was detected in macrophages and not in myofibroblasts (Acloque et al., 2009; Kalluri and Weinberg, 2009, Zeisberg and Neilson, 2009). Several transcription factors (Snail, Twist, Slug, and Id), which regulate migration, activation, and differentiation (functional characteristics of mesenchymal cells) are also displayed by injured epithelial cells, myofibroblasts, and macrophages (Xu et al., 2003; Kalluri and Weinberg 2009). Although the data *in vitro* studies are robust, but in vivo studies lack absolute proof of transition from epithelial to mesenchymal phenotype (Zeisberg and Duffield, 2010).

The role of EMT in the induction of glomerulosclerosis is more controversial (Liu, 2010). Nonetheless, increasing numbers of reports suggest it to be a critical event in induction of various podocyte-mediated disease manifestations (Yang and Liu, 2001;Li et al., 2008; Yadav et al., 2010). For an example, renal biopsy specimens of both diabetic nephropathy and idiopathic focal segmental glomerulosclerosis commonly display podocyte expression of mesenchymal markers such as FSP1, desmin, MMP-9, Snail, and integrin linked kinase (ILK) (Krezler et al., 2001;Li et al., 2008;Yamaguchi et al., 2009); on the other hand, these podocytes often lack their characteristic markers such as neprhin and ZO-1 (Kretzler et al., 2001; Li et al., 2008; Yamaguchi et al., 2009). Similarly, injured podocytes showed upregulation of desmin, vimentin, and nestin (marker of mesenchymal transformation) in a rat model of puromycin anminonucleoside nephropathy (Zou et al., 2006). Besides glomerulosclerosis, podocytes have been demonstrated to undergo EMT in crescentic glomerulonephritis (Moeller et al., 2004). For an example, in an experimental model of Anti-GBM disease, genetically tagged podocytes lost their markers including Wilms tumor protein 1, synaptopodin, nephrin and podocin, and contributed to crescent formation (Moeller et al., 2004). In *in vitro* studies, TGF-β treatment of podocytes induced changes consistent with loss of epithelia characteristics in the form of attenuated expression of the slit diaphragm associated proteins P-cadherin, ZO-1, and nephrin (Li et al., 2008); moreover, TGF-β-treated podocytes displayed markers of mesenchymal transformation in the form desmin, MMP-9, fibronectin, collagen 1 and transcription factor Snail (Yamaguchi et al., 2009).

Since proliferating cells in intra-Bowman's capsule in HIVAN not only show lack or disorganized actin cytoskeleton but also display absence of the characteristic markers of podocytes- synaptopodin and WT1 (Barisoni et al., 1999; Kimmel et al., 2003; Stokes et al., 2006), it is difficult to assign their lineage to podocytes (Dijkman et al., 2006). Nevertheless, because of supracapillary location of the proliferating cells, several investigators suggested that the lineage of the proliferating cells to be either from visceral or parietal epithelial cells (Dijkman et al., 2006, Yadav et al., 2010). In the present study, cells located in the supracapillary region showed expression α-SMA, vimentin, and FSP1-acquirement of mesenchymal phenotype. Since EMT cells are prone to loose attachment and acquire motility, we speculated that the cells located in the supracapillary region were the cells, which might have detached from their basement membranes (either Bowman's capsule or capillary) and rehabilitated themselves in the Bowman's space.

In an *in vitro* model of tubular cell EMT, the role of sirolimus in the blockade of EMT has been attributed to its effect on partial restoration of E-cadherin expression and inhibition of the *de-novo* expression of α-smooth muscle actin (Copeland., 2007). This concept was also supported by another report in cultured human peritoneal mesothelial cells, which demonstrated the inhibitory role of sirolimus for the expression of Snail/ZEB, key transcription factors for repressor of E-cadherin (Aguilera et al., 2005). In the present study sirolimus-treated HIVAN mice not only showed attenuated expression of ZEB1/2 but also showed enhanced expression of E-cadherin. Thus, our findings are consistent with the observations of other investigators (Aguilera et al., 2005; Copeland., 2007).

Enhanced cell proliferation is hall mark of EMT cells, which requires a well geared machinery for protein synthesis (Kalluri and Weinberg 2009; Zeisberg and Neilson, 2009; Zeisberg and Duffield, 2010). Since mTOR is an important cellular pathway for protein synthesis, it is required for cellular proliferation. As regards molecular events are concerned in HIV-induced activation of mTOR pathway, mTORC1 activation proceeds with the sirolimus-sensitive phosphorylation of 4EBP1 which by freeing eIF4E promots the initiation phase of mRNA translation in kidney cells (Rehman et al., 2012). Activation of mTORC1 leads to the phosphorylation of p70S6 kinase, which phosphorylates eIF4B on Ser^{422}. During the initiation phase of translation, eIF4A, a DEAD box protein, functions as a helicase resolving the complexities in 5"UTR which facilitates the scanning of the pre-initiation complex for the AUG codon; eIF4B assists in this activity. Additionally, p70S6 kinase inhibits the activity of eEF2 kinase, a calcium calmodulin–dependent kinase, by phosphorylating it on Thr^{366}; reduced activity of eEF2 kinase contributs to increase in the level of eEF2 dephosphorylated on Thr^{56} resulting in the activation of eEF2. These events stimulate the elongation phase of mRNA translation. Thus, the activation of mTORC1 pathway contributes to the translation of mRNA by stimulating the initiation as well as the elongation phases. By targeting mTORC1 in kidney cells, sirolimus inhibited the two critical pathways in mRNA translation that together promoted protein synthesis (Rehman et al., 2012). Thus, sirolimus-induced protein synthesis in renal cells contributed to antiproliferative activity in general and cells undergoing EMT in particular.

In addition to the inhibition of mTOR pathway, sirlimus might have contributed to the amelioration of renal lesions in multiple ways. Sirolimus has been reported to display several properties which could modulate the effect of HIV infection (43–47]. Roy et al demonstrated that sirolimus inhibited LTR-mediated transcription of HIV (Roy et al., 2002). Thus, it is possible that sirolimus might have down regulated renal tissue HIV gene transcription. Therefore, it may be important to evaluate the effect of sirolimus on renal tissue expression of phlogogenic genes in general, and HIV genes in particular by microarray analysis in Tg26 mice. Recently, Heredia et al demonstrated that sirolimus down regulated CCR5 and caused accumulation of anti-HIV β-chemokines (Heredia et al., 2008).

Moreover, *in vitro* studies, sirolimus enhanced the anti-HIV activity of HIV-entry inhibitors including vivcriviroc, aplaviroc and enfuvirtide (Nicoletti et al., 2009, 2011). In addition, sirolimus attenuated HIV infection in human peripheral blood leukocyte reconstituted SCID mice (Nicoletti et al., 2009). Furthermore, in a recent prospective trial, sirolimus (as a monotherapy) showed significantly better control of HIV and hepatitis C virus replication in HIV patients with liver transplant (Di Benedetto et al., 2010). Thus, it appears that sirolimus not only attenuates HIV replication but also inhibits its entry target cells expressing CCR5.

We propose the following mechanism for the development of HIV-1 induced EMT in HIVAN (Fig. 5A). HIV-1 promotes enhanced expression of Snail/ZEB transcription factors by glomerular and tubular epithelial cells. Since ZEB is a repressor of transcription of E-cadherin, HIV-1-inujued cells display loss of E-cadherin- characteristic epithelial phenotype. The lost epithelial features gear these cells to undergo reverse embryogenesis- display of their original mesenchymal features- expression of α-SMA. Moreover, these cells display other mesenchymal features in the form of detachment from the basement membrane, disorganization of actin cytoskeleton, and secretion of matrix metalloproteinases. The later may lead to the disruption of basement membrane, and thus enhancing their mobilization into adjacent tissues. These acquired characteristics of the altered epithelial cells would allow them to be present in supracapillary, periglomerular, and peritubular positions. Moreover, these cells have now acquired the status of professional collagen producing cells and may thus contribute to the pathogenesis of both glomerular and tubulo-interstitial sclerosis. In contrast, administration of sirolimus (Fig. 5B) would inhibit HIV-1-induced expression of Snail/ZEB, and thus would promote either preservation or restoration of E-cadherin and other epithelial cell characteristics in these cells. Preservation or restoration of epithelial cell characteristics by these cells will limit their unregulated and excessive production of matrix-proteins. Since accumulation of matrix proteins may not entirely dependent on enhanced protein synthesis but would also be contributed by the alteration in the rate of protein degradation, it would be important to study the effect of sirolimus on renal tissue matrix metalloproteinases in future studies.

We conclude that sirolimus attenuated HIVAN phenotype by modulating HIV-1-mediated renal cell EMT induction in HIVAN mice.

Acknowledgments

This work was supported by grant RO1DK084910 and RO1 DK083931 from National Institutes of Health, Bethesda, MD. We are grateful to Prof. Paul E. Klotman, Mount Sinai School of Medicine, New York, for providing a breeding pair of Tg26 mice.

References

1. Acloque H, Adams MS, Fishwick K, Bronner-Fraser M, Nieto MA. Epithelial-mesenchymal transitions: The importance of changing cell state in development and disease. J Clin Invest. 2009; 119:1438–1449. [PubMed: 19487820]
2. Aguilera A, Aroeira LS, Ramirez-Huesca M, Perez-Lozano ML, Cirugeda A, Bajo MA, Del Peso G, Valenzuela-Fernandez A, Sanchez-Tomero JA, Lopez-Cabrera M, Selgas R. Effects of rapamycin on the epithelial-to- mesenchymal transition of human peritoneal mesothelial cells. Int J Artif Organs. 2005; 28:164–169. [PubMed: 15770593]
3. Barisoni L, Kriz W, Munde P, D'Agatim V. The dysregulated podocyte phenotype: a novel concept in the pathogenesis of collapsing idiopathic focal segmental glomerulosclerosis and HIV-associated nephropathy. J Am Soc Nephrol. 1999; 10:51–61. [PubMed: 9890309]
4. Bird JE, Durham SK, Giancarli MR, Gitliz PH, Pandya DG, Dambach DM, Mozes MM, Kopp B. Captopril prevents nephropathy in HIV-transgenic mice. J Am Soc Nephrol. 1998; 9:1441–1447. [PubMed: 9697666]

5. Burns C, Paul SK, Toth IR, Siva L. Effect of angiotensin-converting enzyme inhibition in HIV-associated nephropathy. J Am Soc Nephrol. 1997; 8:1140–1146. [PubMed: 9219164]
6. Copeland JW, Beaumont BW, Merrilees MJ, Pilmore HL. Epithelial-to-mesenchymal transition of human proximal tubular epithelial cells: effects of rapamycin, mycophenolate, cyclosporin, azathioprine, and methylprednisolone. Transplantation. 2007; 83:809–814. [PubMed: 17414716]
7. Di Benedetto F, Di Sandro S, De Ruvo N, Montalti R, Ballarin R. First report on a series of HIV patients undergoing rapamycin monotherapy after liver transplantation. Transplantation. 2010; 89:733–738. [PubMed: 20048692]
8. Dijkman HB, Weenin JJ, Smeets B, Verrijp C, van Kuppevelt TH, Assmann KK, Steenbergen EJ, Wetzels JF. Proliferating cells in HIV and pamidronate-associated collapsing focal segmental glomerulosclerosis are parietal epithelial cells. Kidney Int. 2006; 70:338–344. [PubMed: 16761013]
9. Freedman BI, Kopp JB, Langefeld CD, Genovese G, Friedman DJ, Nelson GW, Winkler CA, Bowden DW, Polla MR. The apolipoprotein L1 (APOL1) gene and nondiabetic nephropathy in African Americans. J Am Soc Nephrol. 2010; 21:1422–1426. [PubMed: 20688934]
10. Guaita S, Puig I, Franci C, Garrido M, Dominguez D, Batlle E, Sancho E, Dedhar S, De Herreros AG, Baulida J. Snail induction of epithelial to mesenchymal transition in tumor cells is accompanied by MUC1 repression and ZEB1 expression. J Biol Chem. 2002; 277:39209–39216. [PubMed: 12161443]
11. Grooteclaes ML, Frisch SM. Evidence for a function of CtBP in epithelial gene regulation and anoikis. Oncogene. 2000; 19:3823–3828. [PubMed: 10949939]
12. Hay D, Zu kA. Transformations between epithelium and mesenchyme: Normal, pathological, and experimentally induced. Am J Kidney Dis. 1995; 26:678–690. [PubMed: 7573028]
13. Heredia A, Latinovic O, Gallo RC, Melikyan G, Reitz M. Reduction of CCR5 with low-dose rapamycin enhances the antiviral activity of vicriviroc against both sensitive and drug-resistant HIV-1. Proc Natl Acad Sci U S A. 2008; 105:20476–20481. [PubMed: 19075241]
14. Hiramatsu N, Hiromura K, Shigehara T, Kuroiwa T, Ideura H, Sakurai N, Takeuchi, Tomioka M, Ikeuchi H, Kaneko Y, Ueki K, Kopp JB, Nojima Y. Angiotensin II type 1 receptor blockade inhibits the development and progression of HIV-associated nephropathy in a mouse model. J Am Soc Nephrol. 2007; 18:515–527. [PubMed: 17229913]
15. Kalluri R, Weinberg RA. The basics of epithelial-mesenchymal transition. J Clin Invest. 2009; 119:1420–1428. [PubMed: 19487818]
16. Kimmel PL, Barisoni L, Kopp JB. Pathogenesis and treatment of HIV-associated renal diseases: lessons from clinical and animal studies, molecular pathologic correlations, and genetic investigations. Ann Intern Med. 2003; 139:214–226. [PubMed: 12899589]
17. Kopp JB, Klotman ME, Adler SH, Bruggeman LA, Dickie P, Marinos NJ, Eckhaus M, Bryant JL, Notkins AL, Klotman PE. Progressive glomerulosclerosis and enhanced renal accumulation of basement membrane components in mice transgenic for human immunodeficiency virus type 1 genes. Proc Natl Acad Sci U S A. 1992; 89:1577–1581. [PubMed: 1542649]
18. Kopp JB, Smith MW, Nelson GW, Johnson RC, Freedman BI, Bowden DW, Oleksyk T, McKenzie LM, Kajiyama H, Ahuja TS, Berns JS, Brigg W, Cho ME, Dart RA, Kimmel PL, Korbet SM, Michel DM, Mokrzycki MH, Schelling JR, Simon E, Trachtman H, Vlahov D, Winkler CA. MYH9 is a major-effect risk gene for focal segmental glomerulosclerosis. Nat Genet. 2008; 40:1175–1184. [PubMed: 18794856]
19. Kretzler M, Teixeira VP, Unschul PG, Cohen CD, Wanke R, Edenhofe I, Mundel, Schlondorff D, Holthofer H. Integrin-linked kinase as a candidate downstream effector in proteinuria. FASEB J. 2001; 15:1843–1845. [PubMed: 11481249]
20. Lan HY. Tubular epithelial-myofibroblast transdifferentiation mechanisms in proximal tubule cells. Curr Opin Nephrol Hypertens. 2003; 12:25–29. [PubMed: 12496662]
21. Li Y, Yang J, Dai C, Wu C, Liu Y. Role for integrin-linked kinase in mediating tubular epithelial to mesenchymal transition and renal interstitial fibrogenesis. J Clin Invest. 2003; 112:503–516. 2003. [PubMed: 12925691]
22. Liu Y. New insights into epithelial-mesenchymal transition in kidney fibrosis. J Am Soc Nephrol. 2010; 21:212–222. [PubMed: 20019167]

23. Li Y, Kang YS, Dai C, Kiss LP, Wen X, Liu Y. Epithelial-to-mesenchymal transition is a potential pathway leading to podocyte dysfunction and proteinuria. Am J Pathol. 2008; 172:299–308. [PubMed: 18202193]
24. Lu TC, He JC, Klotman P. Animal models of HIV-associated nephropathy. Curr Opin Nephrol Hypertens. 2006; 15:233–237. [PubMed: 16609288]
25. Marras D, Bruggeman LA, Ga F, Tanji, Mansukhani MM, Cara A, Ross MD, Gusella G, Benson G, D'Agati VD, Hahn BH, Klotman ME, Klotman PE. Replication and compartmentalization of HIV-1 in kidney epithelium of patients with HIV-associated nephropathy. Nat Med. 2002; 8:522–526. [PubMed: 11984599]
26. Moeller MJ, Soofi A, Hartmann I, Le Hir M, Wiggins R, Kriz W, Holzman LB. Podocytes populate cellular crescents in a murine model of inflammatory glomerulonephritis. J Am Soc Nephrol. 2004; 15:61–67. [PubMed: 14694158]
27. Ng YY, Fan JM, Mu W, Nikolic-Paterson DJ, Yang WC, Huang TP, Atkins RC, Lan Y. Glomerular epithelial-myofibroblast transdifferentiation in the evolution of glomerular crescent formation. Nephrol Dial Transplant. 1999; 14:2860–2872. [PubMed: 10570089]
28. Ng Y, Huang TP, Yang WC, Chen ZP, Yang AH, Mu W, Nikolic-Paterson DJ, Atkins RC, Lan H. Tubular epithelial-myofibroblast transdifferentiation in progressive tubulointerstitial fibrosis in 5/6 nephrectomized rats. Kidney Int. 1998; 54:864–876. [PubMed: 9734611]
29. Nicoletti F, Fagone P, Meroni P, McCubrey J, Bendtzen K. mTOR as a multifunctional therapeutic target in HIV infection. Drug Discov Today. 2011; 16:715–721. [PubMed: 21624501]
30. Nicoletti F, Lapenta C, Donati S, Spada M, Ranazzi A. Inhibition of human immunodeficiency virus (HIV-1) infection in human peripheral blood leucocytes-SCID reconstituted mice by rapamycin. Clin Exp Immunol. 2009; 155:28–34. [PubMed: 19076826]
31. Oldfield MD, Bac LA, Forbes JM, Nikolic-Paterson D, McRobert A, Thalla V, Atkins RC, Osicka T, Jerums G, Cooper ME. Advanced glycation end products cause epithelial-myofibroblast transdifferentiation via the receptor for advanced glycation end products (RAGE). J Clin Invest. 2001; 108:1853–1863. [PubMed: 11748269]
32. Papeta N, Chan KT, Prakash S, Martino J, Kiryluk K, Ballard D, Bruggeman L, Frankel R, Zheng, Klotman PE, Zha H, D'Agati VD, Lifton P, Gharavi AG. Susceptibility loci for murine HIV-associated nephropathy encode trans-regulators of podocyte gene expression. J Clin Invest. 2009; 119:1178–1188. [PubMed: 19381020]
33. Papeta N, Sterken R, Kiryluk K, Kalyesubula R, Gharav AG. The molecular pathogenesis of HIV-1 associated nephropathy: recent advances. J Mol Med. 2011; 89:429–436. [PubMed: 21221512]
34. Rao TK, Friedman EA, Nicastri AD. The types of renal disease in the acquired immunodeficiency syndrome. N Engl J Med. 1987; 316:1062–1068. [PubMed: 3561458]
35. Rehman S, Husain M, Yadav A, Kasinath BS, Malhotra A, Singhal PC. HIV-1 promotes renal tubular epithelial cell protein synthesis: Role of mTOR pathway. Plos One. 2012; 7:e30071. [PubMed: 22253885]
36. Roy J, Paquette JS, Fortin JF, Tremblay MJ. The immunosuppressant rapamycin represses human immunodeficiency virus type 1 replication. Antimicrob Agents Chemother. 2002; 46:3447–3455. [PubMed: 12384349]
37. Stokes MB, Valeri AM, Markowitz G, D'Agati VD. Cellular focal segmental glomerulosclerosis: Clinical and pathologic features. Kidney. Int. 2006; 70:1783–1792. [PubMed: 17021605]
38. Szczech LA, Gupt SK, Habash R, Guasch A, Kalayjian R, Appe, Fields TA, Svetkey LP, Flanagan KH, Klotman PE, Winston JA. The clinical epidemiology and course of the spectrum of renal diseases associated with HIV infection. Kidney Int. 2004; 66:1145–1152. [PubMed: 15327410]
39. Wolf G. Renal injury due to renin–angiotensin–aldosterone system activation of the transforming growth factor-beta pathway. Kidney Int. 2006; 70:1914–1919. [PubMed: 16985515]
40. Wu MJ, Wen MC, Chiu YT, Chio YY, Shu KH, Tang MJ. Rapamycin attenuates unilateral ureteral obstruction-induced renal fibrosis. Kidney Int. 2006; 69:2029–2036. [PubMed: 16732193]
41. Xue C, Plieth D, Venkov C, Xu, Neilso EG. The gatekeeper effect of epithelial-mesenchymal transition regulates the frequency of breast cancer metastasis. Cancer Res. 2003; 63:3386–3394. [PubMed: 12810675]

42. Yadav A, Vallabu S, Kumar D, Ding G, Charney DN, Chander PN, Singhal PC. HIVAN phenotype: consequence of epithelial mesenchymal transdifferentiation. Am J Physiol Renal Physiol. 2010; 298:F734–F744. [PubMed: 20015943]
43. Yamaguchi Y, Iwano M, Toyoda M, Kimura K, Harada K, Nakatani Y, Yoshimoto S, Asai O, Akai Y, Suzuki D, Kanauchi M, Neilson EG, Saito Y. Epithelial-mesenchymal transition as an explanation for podocyte depletion in diabetic nephropathy. Am J Kidney Dis. 2009; 54:653–664. [PubMed: 19615802]
44. Yang J, Liu Y. Dissection of key events in tubular epithelial to myofibroblast transition and its implications in renal interstitial fibrosis. Am J Pathol. 2001; 159:1465–1475. [PubMed: 11583974]
45. Youhua L. Epithelial to Mesenchymal Transition in Renal Fibrogenesis: Pathologic Significance, Molecular Mechanism, and Therapeutic Intervention. J Am Soc Nephrol. 2004; 15:1–12. [PubMed: 14694152]
46. Zeisberg M, Duffield JS. Resolved: EMT produces fibroblasts in the kidney. J Am Soc Nephrol. 2010; 21:1247–1253. [PubMed: 20651165]
47. Zeisberg M, Neilson EG. Biomarkers for epithelial-mesenchymal transitions. J Clin Invest. 2009; 119:1429–1437. 2009. [PubMed: 19487819]
48. Zeisberg M, Hanai J, Sugimoto H, Mammoto T, Charytan, Strutz, Kallur R. BMP-7 counteracts TGFbeta1-induced epithelial-to-mesenchymal transition and reverses chronic renal injury. Nat Med. 2003; 9:964–968. [PubMed: 12808448]
49. Zhong J, Zuo, Ma J, Fog AB, Jolicoeur P, Ichikaw I, Matsusaka T. Expression of HIV-1 genes in podocytes alone can lead to the full spectrum of HIV-1-associated nephropathy. Kidney Int. 2005; 68:1048–1060. [PubMed: 16105035]
50. Zou J, Yaoita E, Watanabe Y, Yoshida Y, Nameta M, Li H, Qu Z, Yamamoto T. Upregulation of nestin, vimentin, and desmin in rat podocytes in response to injury. Virchows Arch. 2006; 448:485–492. [PubMed: 16418842]

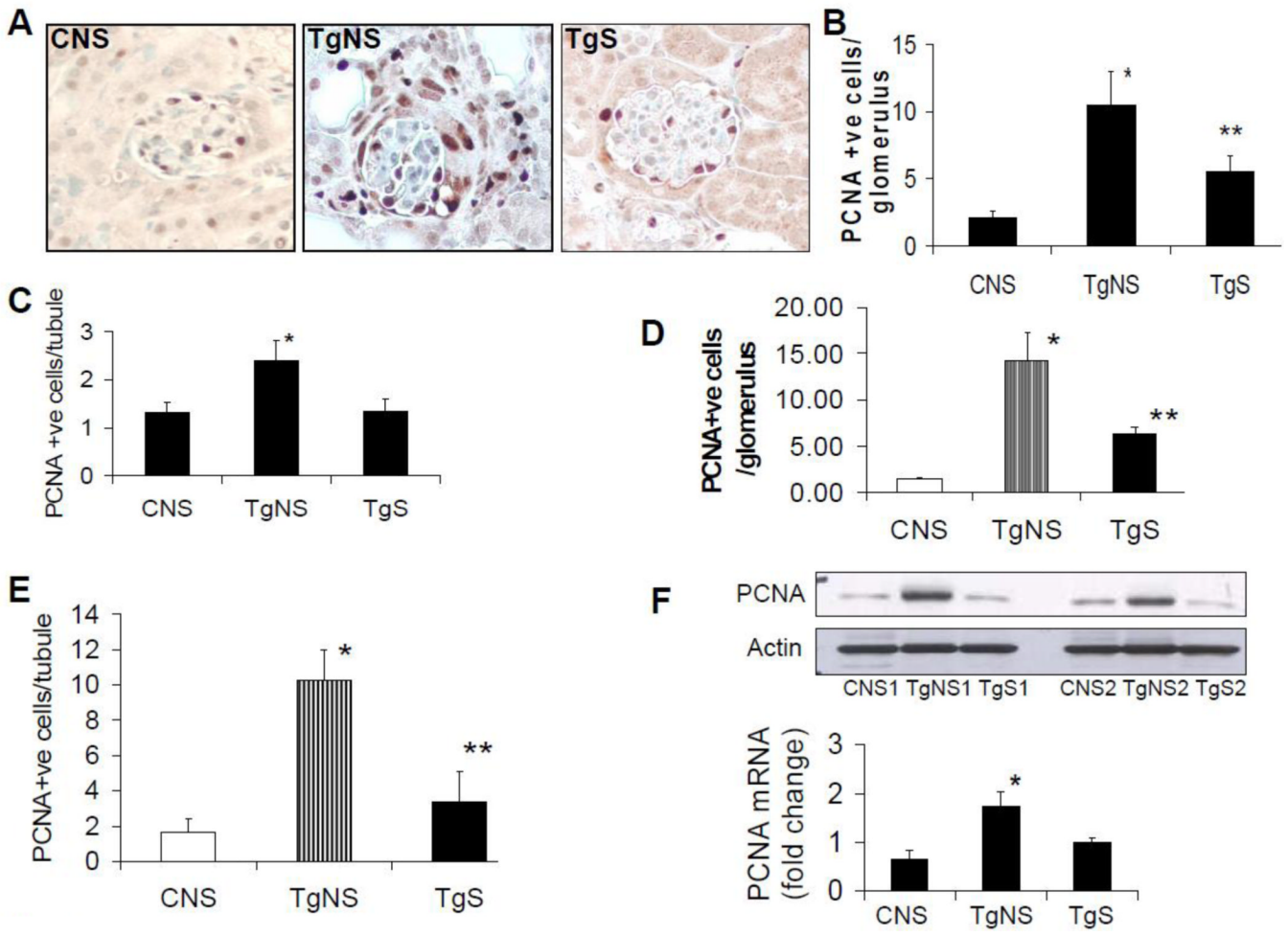

Figure 1. Sirolimus attenuates renal cell proliferative phenotype in HIVAN mice

Renal cortical sections from CNS, TgNS, and TgS from the protocol A (n=6) were immunolabeled for PCNA.

A. Representative microphotographs (Protocol A) of cortical sections of CNS, TgNS, and TgS mice. PCNA +ve cells show dark brown nuclei. X200

B. Cumulative data of mean number of proliferating (+ve PCNA) PECs-PGCs (Protocol A). Number of PCNA +ve cells in 10 random fields was counted and mean number of PCNA +ve cells was calculated per glomerulus. Results (means ± S.D.) are from six mice. *P<0.001 compared with CNS; **P<0.01 compared with TgNS.

C. Cumulative data of mean number of proliferating (+ve PCNA) TCs-PTCs (Protocol A). Number of PCNA +ve cells in 10 random fields was counted and mean number of PCNA +ve cells was calculated per tubule. Results (means ± S.D.) are from six mice. *P<0.01 compared with CNS and TgS.

D. and E. Renal cortical sections from CNS, TgNS, and TgS from the protocol B (n=6) were immunolabeled for PCNA.

D. Cumulative data of mean number of proliferating (+ve PCNA) PECs-PGCs (Protocol B). Number of PCNA +ve cells in 10 random fields was counted and mean number of PCNA +ve cells was calculated per glomerulus. Results (means ± S.D.) are from six mice. *P<0.001 compared with CNS; **P<0.01 compared with TgNS.

E. Cumulative data of mean number of proliferating (+ve PCNA) TCs-PTCs. Number of PCNA +ve cells in 10 random fields was counted and mean number of PCNA +ve cells was

calculated per tubule. Results (means ± S.D.) are from six mice. *P<0.001 compared with CNS; **P<0.01 compared with TgNS.

F. Sirolimus attenuates renal tissue expression of PCNA in HIVAN mice

The upper panel. Proteins were extracted from renal cortical tissues of CNS (1 and 2), TgNS (1 and 2) and TgS (1 and 2) (Protocol A). Western blots were prepared and probed for PCNA, and actin. The upper lane shows renal tissue expression of PCNA by CNS, TgNS, and TgS. The lower lane shows renal tissue expression of actin under the same conditions. The lower panel. Total RNA from renal cortical tissues was isolated from three CNS, TgNS, and TgS. RNAs were evaluated for PCNA expression by real time PCR studies and fold of change compared to control was calculated.

*P<0.01 compared with CNS and TgS

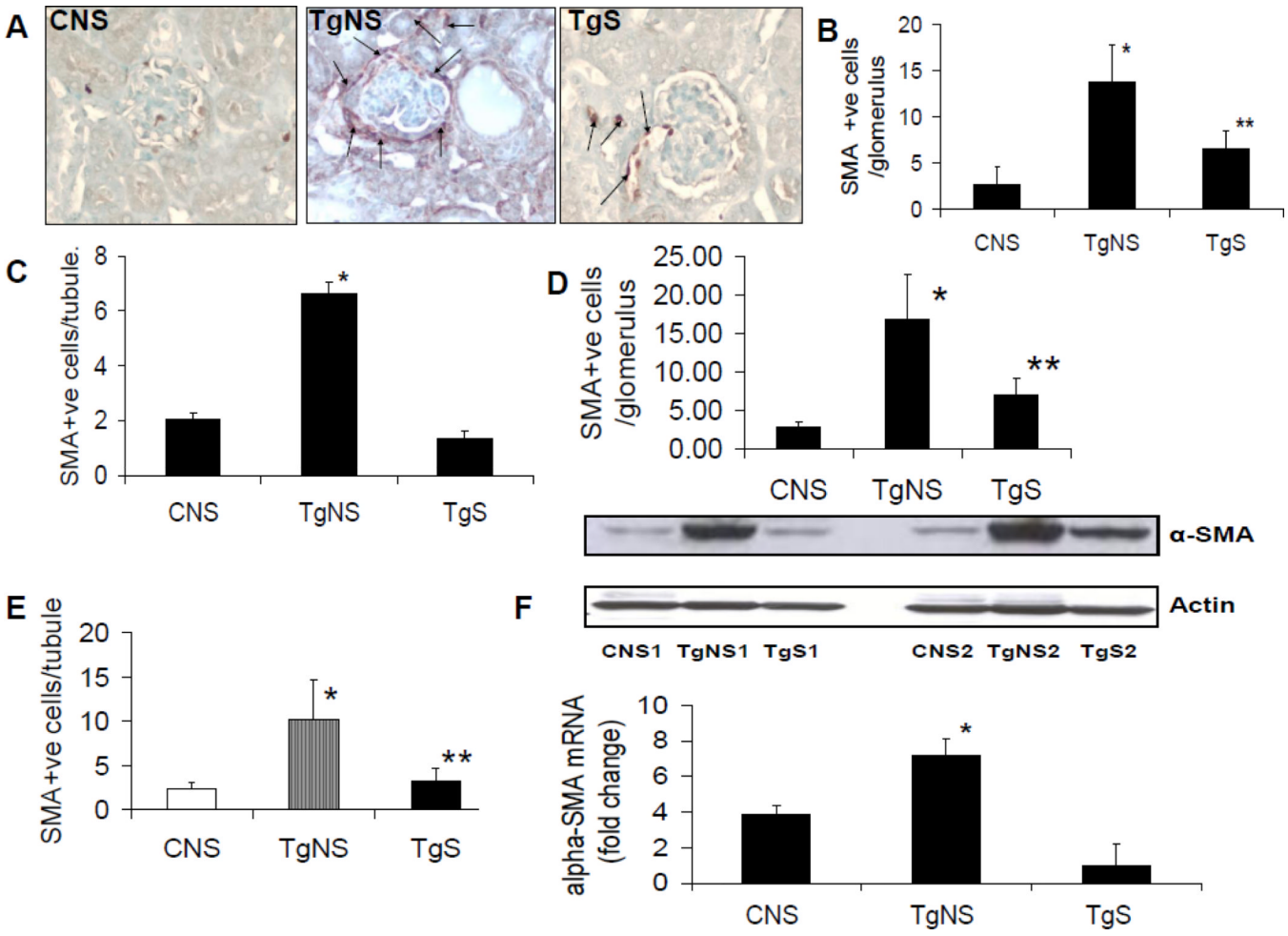

Figure 2. Sirolimus diminishes renal cell expression of α-SMA in HIVAN mice

Renal cortical sections from CNS, TgNS, and TgS from the protocol A (n=6) were immunolabeled for α-SMA.

A. Representative microphotographs of cortical sections of CNS, TgNS, and TgS mice. α-SMA +ve cells show dark brown cytoplasmic staining. X200

B.Cumulative data of mean number of proliferating α-SMA +ve PECs-PGCs. Number of α-SMA +ve cells in 10 random fields was counted and mean number of α-SMA +ve cells per glomerulus was calculated (protocol A). Results (means ± S.D.) are from six mice. *P<0.001 compared with CNS; **P<0.05 compared with TgNS.

C. Cumulative data of mean number of α-SMA +ve TCs-PTCs. Number of α-SMA +ve cells in 10 random fields was counted and mean number of α-SMA +ve/tubule was calculated (Protocol A). Results (means ± S.D., n=6). *P<0.05 compared with CNS and TgS.

D. Cumulative data of mean number of α-SMA +ve PECs-PGCs. Number of α-SMA +ve cells in 10 random fields (Protocol B) was counted and mean number of α-SMA +ve cells/ glmerulus was calculated. Results represent means ± S.D. (n=6). *P<0.001 compared with CNS; **P<0.01 compared with TgNS.

E. Cumulative data of mean number of α-SMA +ve TCs-PTCs. Number of α-SMA +ve cells in 10 random fields was counted and mean number of α-SMA +ve cells per tubule was calculated (Protocol B). Results (means ± S.D.) are from six mice. *P<0.01 compared with CNS; **P<0.05 compared with TgNS.

F. Sirolimus attenuates renal tissue expression of α-SMA in HIVAN mice

Renal cortical tissue RNA was isolated from three CNS, TgNS, and TgS. RNAs were evaluated for α-SMA expression by real time PCR studies and fold of change was calculated (lower panel). *P<0.01 compared with CNS and TgS. Proteins were extracted from renal cortical tissues of CNS (1 and 2), TgNS (1 and 2) and TgS (1 and 2). Western blots were prepared and probed for α-SMA, and actin (upper panel). The upper lane shows renal tissue expression of α-SMA by CNS, TgNS, and TgS. The lower lane shows renal tissue expression of actin under the same conditions.

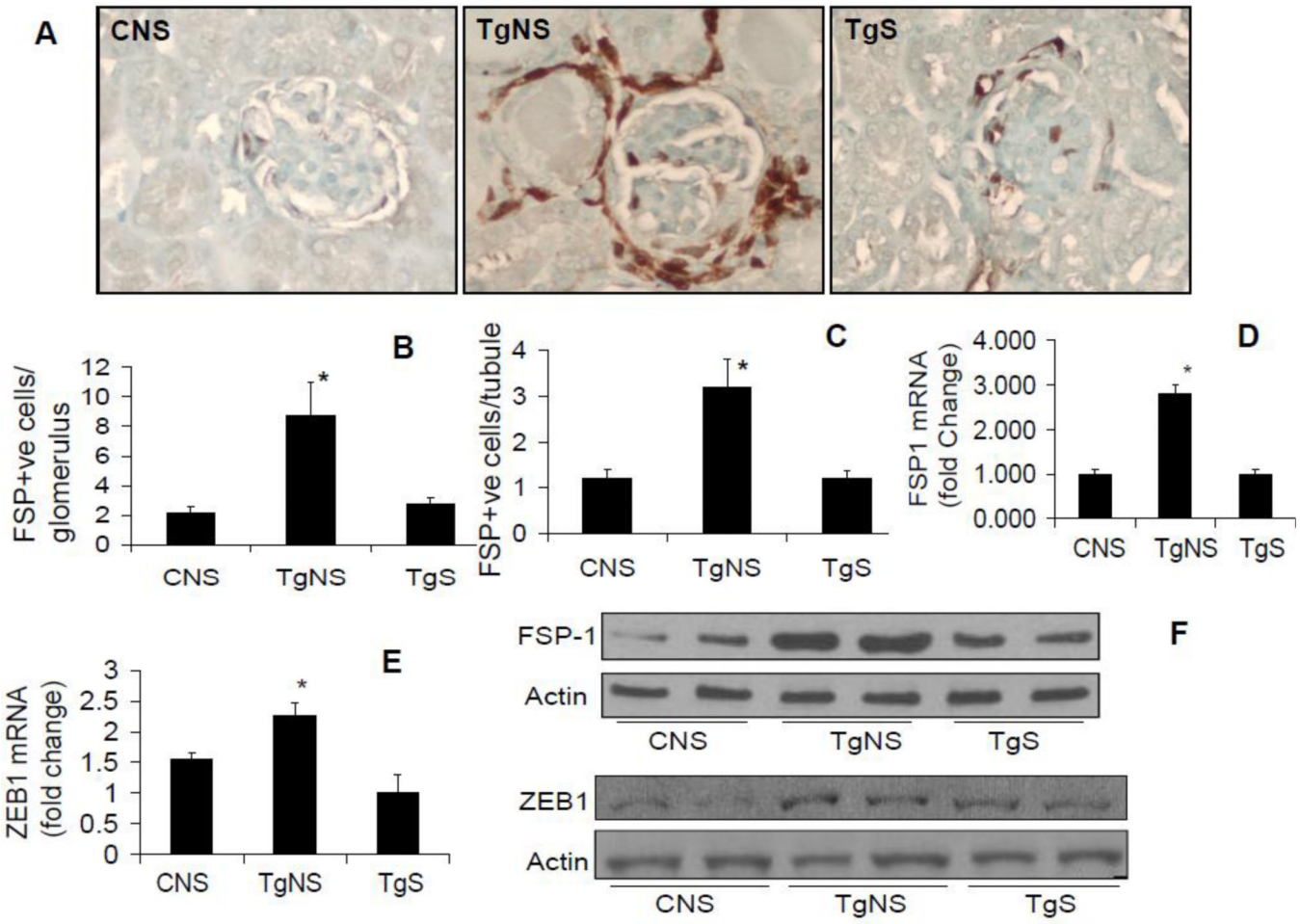

Figure 3. Sirolimus attenuates renal cell FSP1 expression in HIVAN mice

Renal cortical sections from CNS, TgNS, and TgS from the protocol A (n=6) were immunolabeled for FSP1.

A. Representative microphotographs of cortical sections of CNS, TgNS, and TgS. FSP1 +ve cells show dark cytoplasmic staining. X200

B. Cumulative data of mean number of FSP1 +ve PECs-PGCs. Number of FSP1 +ve cells in 10 random fields was counted and mean number of FSP1 +ve cells/glomerulus was calculated (Protocol A). Results (means ± S.D.) are from six mice. *P<0.001 compared with CNS and TgS.

C. Cumulative data of mean number of FSP1 +ve TCs-PTCs. Number of FSP1 +ve cells in 10 random fields was counted and mean number of FSP1 +ve cells/tubule was calculated (Protocol A). Results (means ± S.D.) are from six mice. *P<0.01 compared with CNS and TgS.

D. Sirolimus attenuates renal tissue expression of FSP-1 in HIVAN mice

Renal cortical tissue RNA was isolated from three CNS, TgNS, and TgS. RNAs were evaluated for FSP1 expression by real time PCR studies and fold of change was calculated. *P<0.001 compared with CNS and TgS.

E. Sirolimus attenuates renal tissue mRNA expression of ZEB1 in HIVAN mice.

Total RNA was extracted from renal cortical tissues RNA of three CNS, TgNS, and TgS. RNAs were probed for ZEB1 expression by real time PCR studies and fold of change compared to control was calculated. *P<0.01 compared with CNS and TgS.

F. Sirolimus attenuates FSP-1 and ZEB1 expression in HIVAN mice

Proteins were extracted from two CNS, TgNS and TgS mice. Immunoblots were probed for FSP-1 and ZEB1. The same blots were stripped and reprobed for Actin. Representative gels are shown.

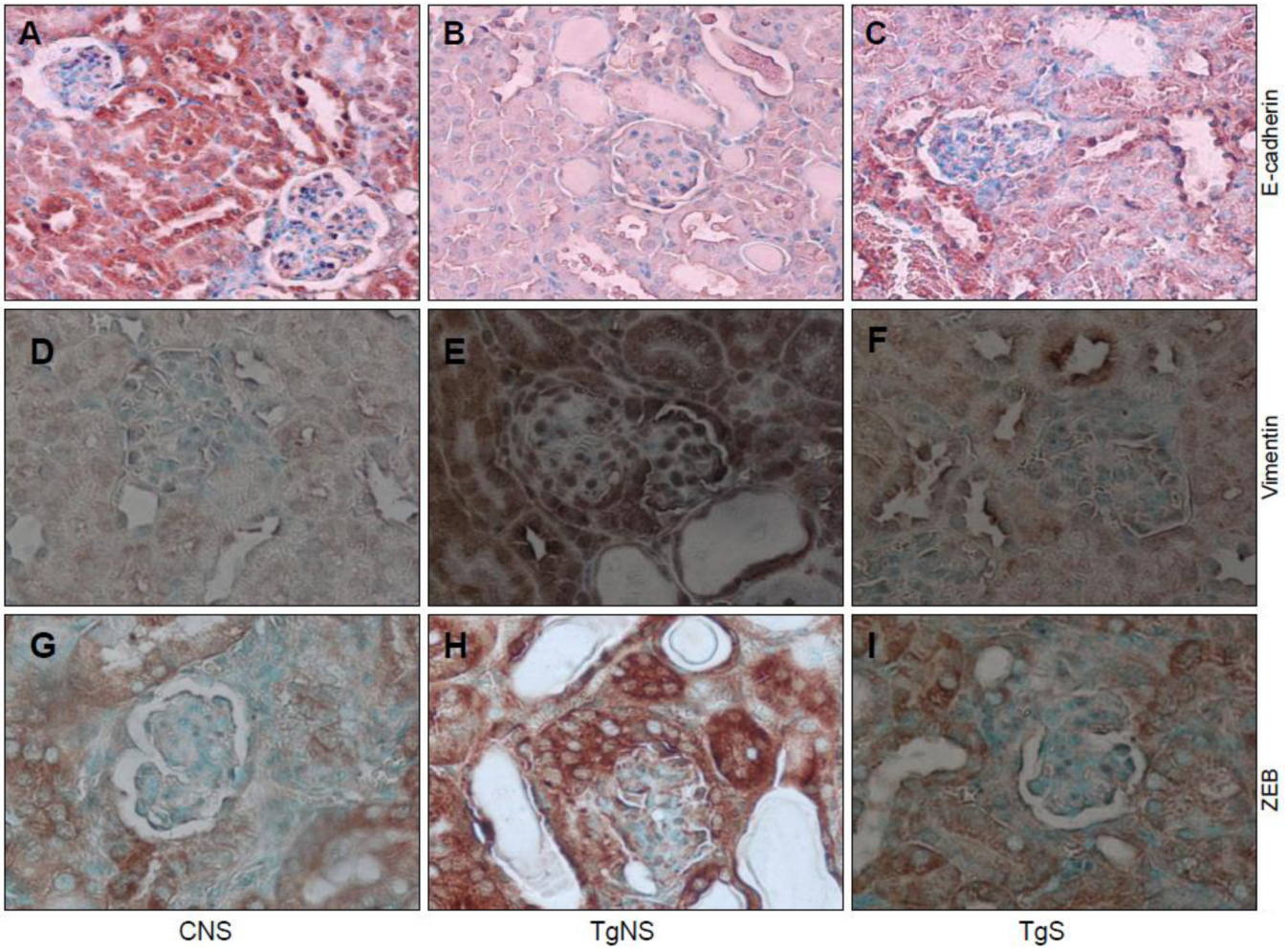

Figure 4. Sirolimus modulates renal cell expression of E-cadherin, vimentin, and ZEB1/2 in HIVAN mice

Renal cortical sections from CNS, TgNS, and TgS from the protocol A (n=6) were immunolabeled for E-cadherin, vimentin, and ZEB1/2.

A–C. Representative microphotographs of cortical sections of CNS, TgNS, and TgS labeled for E-cadherin. Renal epithelia in CNS (A) and TgS (C) showed +ve staining (dark brown, cytoplasmic) for E-cadherin; whereas, renal cells in TgNS (B) showed diminished staining for E-cadherin. X100

D–F. Representative microphotographs of cortical sections of CNS, TgNS, and TgS immunolabeled for vimentin. Renal epithelia in TgNS (E) showed +ve staining (brown, cytoplasmic) for vimentin; whereas, renal cells in CNS (D) and TgS (E) showed attenuated staining for vimentin. X100

G–I. Representative microphotographs of cortical sections of CNS, TgNS, and TgS immunolabeled for ZEB1/2. Renal epithelia in TgNS (E) showed +ve staining (brown, cytoplasmic) for ZEB1/2; whereas, renal cells in CNS (D) and TgS (E) showed diminished staining for ZEB1/2. X100

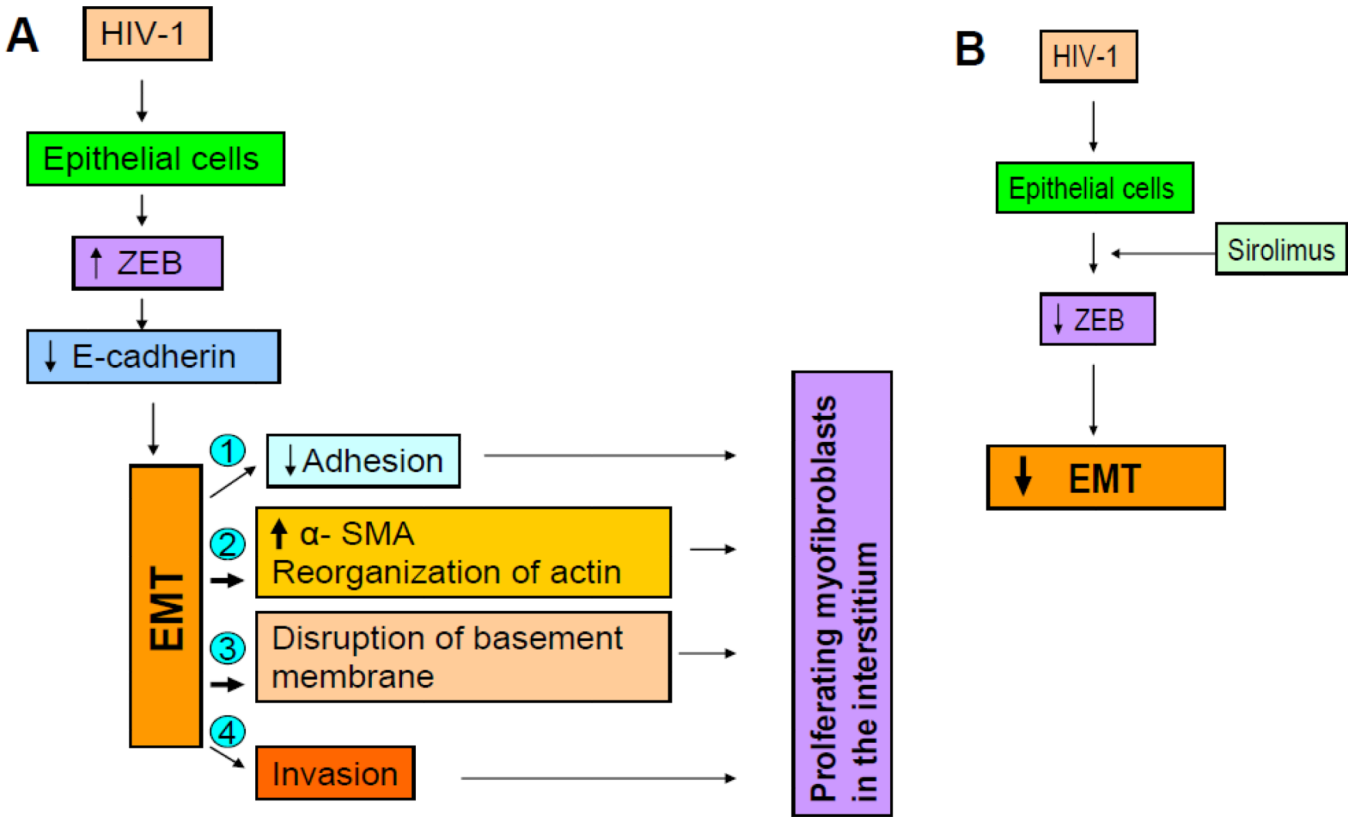

Figure 5.

A. Proposed scheme showing role of HIV-1 in the induction of EMT in HIVAN.

B. Proposed mechanism of sirolimus in the attenuation of EMT in HIVAN.